Superlinear photovoltaic effect in Si nanocrystals based metal-insulator-semiconductor devices

S. Prezioso,[1,a)] S. M. Hossain,[1,b)] A. Anopchenko,[1] L. Pavesi,[1] M. Wang,[2] G. Pucker,[2] and P. Bellutti[2]
[1]*Dipartimento di Fisica, Laboratorio di Nanoscienze, Università di Trento, Via Sommarive 14, 38100 Povo (Trento), Italy*
[2]*Microtechnologies Laboratory, Fondazione Bruno Kessler, Via Sommarive 18, 38100 Povo (Trento), Italy*

(Received 8 September 2008; accepted 24 January 2009; published online 12 February 2009)

Superlinear-variation in short circuit photocurrent with increasing incident optical power has been observed in metal-insulator-semiconductor structures having a silicon rich oxinitride active layer containing silicon nanocrystals. A model has been elaborated where an internal gain mechanism explains the superlinear photovoltaic effect. The internal gain mechanism is due to secondary carrier generation (SCG) from sub-bandgap levels in the nanocrystal. SCG is caused by impact excitation from the photogenerated conduction band electrons. The sub-bandgap levels are associated to traps formed at the dielectric/Si-nanocrystals interface. © *2009 American Institute of Physics.*
[DOI: 10.1063/1.3081410]

In recent years, silicon nanocrystals (Si-ncs) have been employed in many electronic devices such as high quality memory devices[1–4] and electroluminescent devices.[5–7] Recent results have shown the possibility of using nanocrystalline silicon to develop third generation photovoltaics (PV),[8–10] where the theoretical efficiency is well beyond the Shockley–Queisser[11] efficiency limit. One way is to exploit the multiple exciton generation (MEG) induced by high energy solar photons inside the active region of solar cells.[12,13] A first demonstration of MEG in nanocrystalline silicon has been reported in Ref. 14 when the ncs are in colloidal form. In the present work, PV effect was investigated in devices with a metal-insulator-semiconductor (MIS) structure, where the insulator is a silicon rich oxinitride (SRON) matrix containing Si-ncs: photogenerated electron-hole (e-h) pairs in Si-ncs by high energy photons trigger secondary carrier generation (SCG) from nitrogen related trap states.

A SRON layer of 50 nm thickness was grown on *p*-type (12–18 Ω cm) Si substrate by plasma enhanced chemical vapor deposition. The SRON was subsequently annealed at 1050 °C for 60 min to form Si-ncs. By controlling the ratio of SiH_4, N_2O, and NH_3 fluxes, 54 at. % of Si and 8 at. % of N were obtained from the SRON film. A 30 nm thick *n*-type polycrystalline silicon (poly-Si) gate layer was deposited on the SRON layer, followed by deposition of an Al grid (500 nm thick). The metal free region of the poly-Si layer was covered by an antireflective coating (ARC, a 50 nm thick Si_3N_4 layer and a 120 nm thick SiO_2 layer). A schematic cross section of the device is depicted in the inset of Fig. 1. Device area was 320×320 μm^2. Sample illumination was realized with both the 488 nm Ar^+ laser and the 633 nm He–Ne laser line. In addition, infrared (IR) illumination was provided by a tungsten lamp filtered with a 1200 nm long wave pass filter to identify the sub-bandgap contributions to the photoresponse of the sample.

Short circuit current I_{sc} has been studied as a function of incident optical intensity of both visible wavelengths (488 and 633 nm) (Fig. 1). A comparison with the 633 nm short circuit current flowing through silicon rich oxide (SRO) layers is reported; that will be discussed later on. A superlinear-variation with incident intensity is observed, which eventually gets linear and then sublinear. This interesting result can be explained considering that

(i) Si-ncs are present in the active device layer with dimensions larger than 5 nm,[15] the corresponding bandgap estimated from photoluminescence (PL) spectra[16] being lower than 1.4 eV;
(ii) the dielectric/Si-nc interfaces are characterized by nitrogen related sub-bandgap trap states that cause hysteresis in the IV characteristics[16] and IR absorption lines;[17] and
(iii) a prevalent current of electrons flows through the SRON layer,[17] the holes being impeded by their low mobility and large energy barriers.

The fact that short circuit current is lower if measured at 488 nm excludes any mechanism that invokes a release of

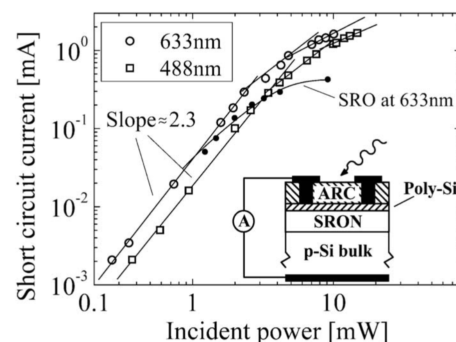

FIG. 1. Variation in short circuit current as a function of incident power intensity for two different wavelengths (488 nm, empty square dots, and 633 nm, empty circles). 633 nm short circuit current through SRO is reported for comparison (filled circles). Inset: schematic cross section of the device.

[a)]Electronic mail: stefanoprezioso@gmail.com. Present address: Department of Physics, University of L'Aquila, L'Aquila, Italy.
[b)]Present address: Department of Physics, Bengal Engineering and Science University, Shibpur, India.

 © 2009 American Institute of Physics

Author complimentary copy. Redistribution subject to AIP license or copyright, see http://apl.aip.org/apl/copyright.jsp

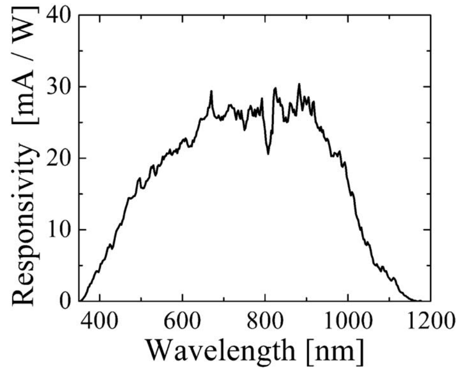

FIG. 2. Spectral response of devices having SRON active layers.

permanently trapped charge under ultraviolet (UV) illumination, where the PV effect induced by 488 or 633 nm illumination should represent a tail of the UV process, whose contribution should weaken as the wavelength increases. This conclusion is supported by the spectral response (Fig. 2) that becomes negligible under UV illumination. In Fig. 3, the proposed model is schematized in a no-bias band diagram configuration: the emphasized intrinsic band bending is responsible for I_{sc}. When a 488 or 633 nm photon is absorbed by the active layer, generating an e-h pair inside a Si-nc [Fig. 3(a)], the photogenerated hole is most likely trapped within the nc, whereas the photogenerated electron either contributes to the short circuit current [process labeled 1 in Fig. 3(a)] or recombines with the trapped hole radiatively (process labeled 2) or gets trapped at the dielectric/Si-nc interface (process labeled 3). The electron trapping is the key process in our model. In fact, when a second photon is absorbed by the same Si-nc [Fig. 3(b)], a fourth option is possible: since the energy of the absorbed photon is much larger than the nc bandgap, the photogenerated electron has extra kinetic energy that can be released by impact excitation of the trapped electron[18] [Fig. 3(b)]. This mechanism generates a current of secondary carriers (J_{SCG}).

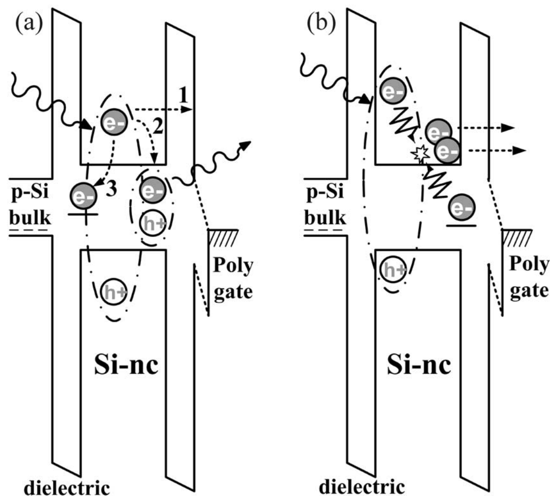

FIG. 3. Schematic energy diagram of the active layer under short circuit bias. (a) Primary photoexcitation process where an e-h pair is generated and where the photoexcited electron either (1) contributes to the short circuit current or (2) recombines or (3) is trapped. (b) Secondary photoexcitation process where a photogenerated electron detraps a sub-bandgap electron and both contribute to the short circuit current.

It is easy to show that J_{SCG} increases superlinearly with the incident light intensity. In fact, let us call n_{ts}^f the density of filled trap states; then J_{SCG} is proportional to $-dn_{ts}^f/dt$ integrated on the whole active layer thickness d,

$$J_{SCG} = \int_d q\left(-\frac{dn_{ts}^f}{dt}\right)dx \approx q\ d\left(-\frac{dn_{ts}^f}{dt}\right), \tag{1}$$

where q is the electronic charge and a constant detrapping rate throughout the SRO layer is assumed for simplicity. $-dn_{ts}^f/dt$ is proportional to n_{ts}^f and to the density of photoexcited hot electrons, which in turn is proportional to the incident photon flux J_{ph},

$$-\frac{dn_{ts}^f}{dt} \propto J_{ph} n_{ts}^f. \tag{2}$$

This law expresses the rate of secondary carriers emitted from the filled traps. Using (1) and (2),

$$J_{SCG} \propto J_{ph} n_{ts}^f. \tag{3}$$

The filled traps easily get emptied even with intrinsic band bending conditions (no bias) because of the high mobility of electrons. Moreover, traps are filled exclusively when a photogenerated electron relaxes into a sub-bandgap level [process 3 in Fig. 3(a)]. This means that the average number n_{ts}^f of filled trap states involved in the SCG process depends on the e-h pair generation rate and, in particular, it is proportional to J_{ph} ($n_{ts}^f \propto J_{ph}$). Thus, (3) leads to a quadratic dependence of J_{SCG} on J_{ph},

$$J_{SCG} \propto J_{ph}{}^2. \tag{4}$$

The experimental behavior reported in Fig. 1 (slope $\cong 2.3$) is consistent with the theoretical prediction (slope $=2$). The saturation of J_{SCG} at high values of J_{ph} comes from the saturation of the trap states, n_{ts}^f being a larger and larger fraction of the total trap state density n_{ts} ($n_{ts}^f = \beta n_{ts}$, with $\beta \leq 1$) as J_{ph} increases; complete saturation is reached when $n_{ts}^f = n_{ts}$. Furthermore, repeating the experiment with devices having SRO active layers and focusing the analysis on the saturation conditions, J_{SCG} has been found to be 3.5 times lower where the nitrogen content has been decreased by 50% (Ref. 19) (Fig. 1), confirming that the involved traps are related to the presence of nitrogen, n_{ts} being strongly dependent on the nitrogen content. A further support to this model comes from Fig. 4(a). Here, the photocurrent I_{ph} as a function of the applied voltage is reported. $I_{ph} = I_L - I_D$, where I_L is the current measured under illumination and I_D the one measured in dark conditions. Measurements are reported for different illumination conditions and under reverse bias (negative voltage on the p-type substrate), where the device presents a photodiode-like behavior. In Fig. 4(a) we compare I_{ph} measured in two different illumination conditions: when only visible light is used (7 mW, 633 nm, I_{ph}^{633}) and when both visible and IR light are used (7 mW, 633 nm and 3 mW IR, I_{ph}^{633+IR}). I_{ph}^{633+IR} is larger than I_{ph}^{633} by about 10% in short circuit condition and by 50% at -5 V. Note that the IR light source was filtered at 1200 nm to have photons with energies well below both the Si-nc and the Si-bulk bandgaps. Hence, the extra photocurrent ($\Delta I = I_{ph}^{633+IR} - I_{ph}^{633}$) can be exclusively attributed to the SCG from the sub-bandgap levels populated by IR irradiation. Note that to have the photocurrent enhancement, both visible and IR illuminations are required.

Author complimentary copy. Redistribution subject to AIP license or copyright, see http://apl.aip.org/apl/copyright.jsp

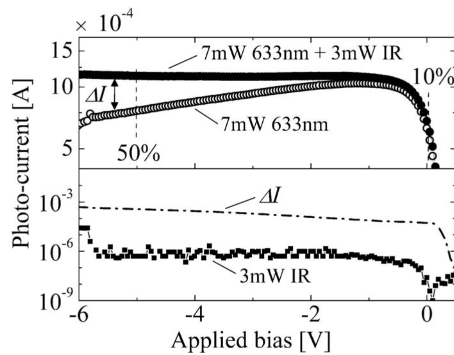

FIG. 4. (a) Photocurrent vs applied bias measured under 7 mW, 633 nm illumination (empty circles) and under both 7 mW, 633 nm and 3 mW IR ($\lambda > 1200$ nm) illumination (filled circles). (b) Photocurrent enhancement (ΔI) caused by IR illumination and visible illumination (dashed line) and photocurrent under solely IR illumination (square dots) vs applied bias.

Indeed, I_{ph} measured under solely IR illumination (I_{ph}^{IR}) is compared to ΔI in Fig. 4(b). I_{ph}^{IR} is more than two orders of magnitude smaller than ΔI. This excludes thermal activation of carriers as a result of device heating, the heat yielded by the same IR beam (3 mW) affecting differently the electric transport, while it should depend exclusively on the incident optical power. Moreover, this means that filled trap states are not enough to yield large photocurrent; one needs the assistance of hot electrons to detrap carriers from the trap states. Finally, the large ΔI measured in short circuit condition shows that this SCG mechanism can be usefully employed to increase the efficiency of solar cells by exploiting sub-bandgap photons present in the solar spectrum, where both IR and visible photons are present simultaneously.

In conclusion, a superlinear PV effect has been observed in MIS-SRON structures containing Si-ncs. It has been attributed to SCG from subnanocrystal bandgap trap states located at the dielectric/Si-nc interface and related to the presence of nitrogen in the dielectric matrix. With illumination of solely high energy photons, SCG works as a mechanism that recovers electrons relaxed into the sub-bandgap states. When sub-bandgap excitons are generated directly by IR illumination, SCG works as an amplification mechanism for the IR photocurrent component. For this reason, the adoption of SRON in silicon based solar cells could offer the opportunity to exploit efficiently the sub-bandgap photons present in the solar spectrum.

This research was commissioned by Optoelettronica Italia S.r.l. within a project on photovoltaics named HCSC financed by PAT. One of the authors (S.M.H.) thanks DST, Govt. of India for awarding BOYSCAST fellowship.

[1]S. Tiwari, F. Rana, H. Hanafi, A. Hartstein, E. F. Crabbe, and K. Chan, Appl. Phys. Lett. **68**, 1377 (1996).
[2]S. Tiwari, J. A. Wahl, H. Silva, F. Rana, and J. J. Welser, Appl. Phys. A: Mater. Sci. Process. **71**, 403 (2000).
[3]M. Porti, M. Avidano, M. Nafria, X. Aymerich, J. Carreras, O. Jambois, and B. Garrido, J. Appl. Phys. **101**, 064509 (2007).
[4]T. Z. Lu, M. Alexe, R. Scholz, V. Talalaev, R. J. Zhang, and M. Zacharias, J. Appl. Phys. **100**, 014310 (2006).
[5]S. Ossicini, L. Pavesi, and F. Priolo, *Light Emitting Silicon for Microphotonics*, Springer Tracts in Modern Physics (Springer, Berlin, 2003), Vol. 194.
[6]F. Iacona, A. Irrera, G. Franzo, D. Pacifici, I. Crupi, M. Miritello, C. D. Presti, and F. Priolo, IEEE J. Sel. Top. Quantum Electron. **12**, 1596 (2006).
[7]R. J. Walters, J. Carreras, T. Feng, L. D. Bell, and H. A. Atwater, IEEE J. Sel. Top. Quantum Electron. **12**, 1647 (2006).
[8]A. J. Nozik, Physica E (Amsterdam) **14**, 115 (2002).
[9]M. A. Green, Physica E (Amsterdam) **14**, 65 (2002).
[10]M. A. Green, Prog. Photovoltaics **9**, 123 (2001).
[11]W. Shockley and H. J. Queisser, J. Appl. Phys. **32**, 510 (1961).
[12]P. T. Landsberg, H. Nussbaumer, and G. Willeke, J. Appl. Phys. **74**, 1451 (1993).
[13]S. Kolodinski, J. H. Werner, T. Wittchen, and H. J. Queisser, Appl. Phys. Lett. **63**, 2405 (1993).
[14]M. C. Beard, K. P. Knutsen, P. Yu, J. M. Luther, Q. Song, W. K. Metzger, R. J. Ellingson, and A. J. Nozik, Nano Lett. **7**, 2506 (2007).
[15]C. Delerue, G. Allan, and M. Lannoo, J. Lumin. **80**, 65 (1998).
[16]S. Prezioso, A. Anopchenko, Z. Gaburro, L. Pavesi, G. Pucker, L. Vanzetti, and P. Bellutti, J. Appl. Phys. **104**, 063103 (2008).
[17]S. M. Hossain, A. Anopchenko, S. Prezioso, L. Ferraioli, L. Pavesi, G. Pucker, P. Bellutti, S. Binetti, and M. Acciarri, J. Appl. Phys. **104**, 074917 (2008).
[18]D. Timmerman, I. Izeddin, P. Stallinga, I. N. Yassievich, and T. Gregorkiewicz, Nat. Photonics **2**, 105 (2008).
[19]Device specifications are reported in Ref. 16 where the cited samples are addressed as Γ3*N* (SRON) and Γ3 (SRO), respectively.

Author complimentary copy. Redistribution subject to AIP license or copyright, see http://apl.aip.org/apl/copyright.jsp